

Study On Selection of Fuel Cell Power Configuration for Heavy Duty Truck Applications Using GT-Simulation

S. Karthikeyan^{1*}, Gopi Sankar M.²

Abstract

Today, there are a plethora of fuel cell types available on the market with a wide range of applications, including transportation, stationary power, portable power, and emergency backup power. Among these fuel cells, proton exchange membrane fuel cells (PEMFC) have the potential for use in automotive applications due to their low operating temperatures as well as high power density. Furthermore, these PEMFC power sources are also available in various power ranges and capacities for diverse vehicle applications. However, a challenging task is the selection of optimised fuel cell power configurations for heavy-duty truck applications due to cost sensitivity and competitiveness in the Indian market. Therefore, considering the above scenario, for finalising the design specifications of the fuel cell system, a simulation study to understand PEMFC performance based on the vehicle operating conditions is significant to determining the suitable fuel cell power capacity for truck applications. Accordingly, a truck fuel cell electric vehicle model with > 30 to 40 tonnes of payload capacity is developed using GT-SUITE software for a performance simulation study. Based on the simulation results, a 100 kW fuel cell power is selected for the given truck payload capacity, and their performances are discussed in this paper.

Keywords: PEM-fuel cell, truck, design, simulation, greenhouse gas

INTRODUCTION

The use of internal combustion engines, with their highly potent gases, contributes significantly to the rise in pollution levels. Further, increased human practises also resulted in an increase in greenhouse gases in the atmosphere over the last 150 years. [1], as shown in Figure 1. Due to this rapid rise in engine pollution, all life on earth is under the duress of global warming and ozone depletion concerns. Particularly, commercial vehicles are one of the sources and have a significant contribution to these on-road emissions. This is due to the fact that large capacity engines are used to transport large loads over long distances. In addition to CO₂ emissions and diesel fuel's enormous cost, the vehicle manufacturers face enormous pressure to innovate new products with alternate energy technology at a lower cost and with a considerably shorter development time for the commercial vehicles (CVs).

Hence, the need for greener technology in transportation becomes momentous. One such green solution is the development of a fuel cell electric vehicle [1–2]. For this reason, the significance of hydrogen fuel cell technology with a polymer electrolyte membrane is contrived. Accordingly, the conversion of these combustion engine-powered commercial vehicles (CVs) to fuel cell electric power trains will play a large role in reducing harmful emissions. This FC technology also offers many benefits, like high energy efficiency, convenient operation, and environmentally friendly features for CVs. These

*Author for Correspondence

S. Karthikeyan
E-mail: dr.karthikeyan@ashokleyland.com

¹Head, Fuel Cell Department, Ashokleyland, Chennai, India
²Vice President, Department of Advanced Engineering, Ashokleyland, Chennai, India

Received Date: December 07, 2023
Accepted Date: December 20, 2023
Published Date: January 23, 2024

Citation: S. Karthikeyan, Gopi Sankar M. Study on Selection of Fuel Cell Power Configuration for Heavy Duty Truck Applications Using GT-Simulation. International Journal of I.C. Engines and Gas Turbines. 2023; 9(2): 10–29p.

Fuel cells are electrochemical cells that convert the chemical energy of a fuel such as hydrogen into electricity [2]. This conversion takes place through a couple of redox reactions between fuel and oxygen within a cell [3], and a fuel cell is capable of continuously producing electricity as long as oxygen and fuel are supplied [4].

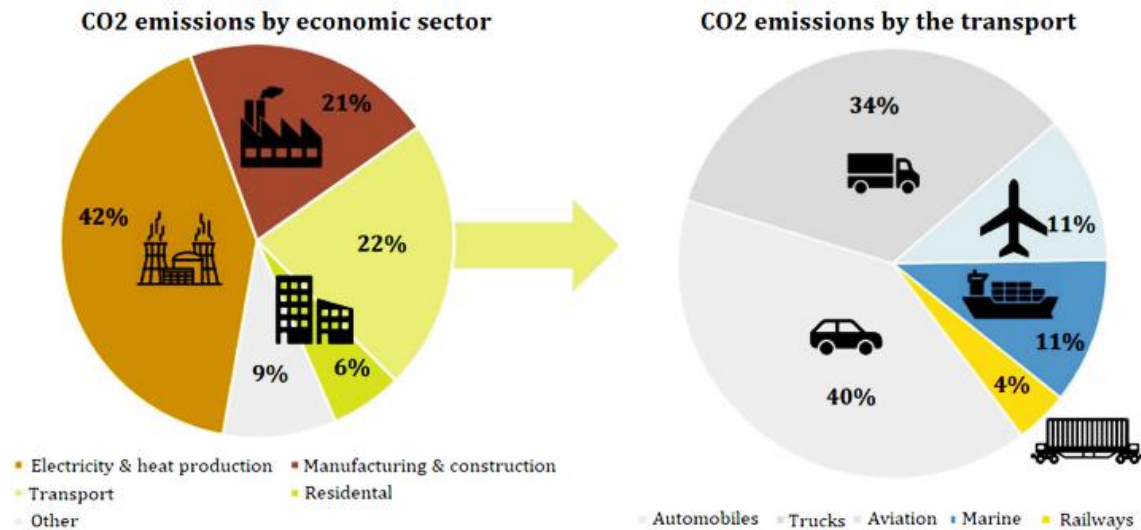


Figure 1. Global greenhouse gas from different commercial sector [1].

Table 1. Comparison of fuel cell types for concept selection process [9].

Fuel Cell	Temperature (°C)	Fuel	Electrolyte	Uses	Electrical efficiency (%)
PEMFC	40-90	H ₂ (~99%)	Polymer	Vehicles, small generators	40-60
AFC	40-250	H ₂ (100%)	Potassium Hydroxide	Outer space	60-70
DMFC	60-130	Methanol	Polymer	Vehicles, small appliances	~40
PAFC	150-220	H ₂ (~99%)	Phosphoric Acid	Power plants combined heat and power	36-42
MCFC	600-700	CH ₄ , H ₂ , CO	Molten Carbonate	Power plants, combined heat and power	40-50
SOFC	600-100	CH ₄ , H ₂ , CO	Solid Oxide	Power plants combined heat and power	50-60
<ul style="list-style-type: none"> Only fuel to electrical efficiency is considered; by –product heat is ignored 					
Non-noble metals		Noble metals/non-noble metals		Noble metals	

Overall, there are six major types of fuel cells that could be categorized based on fuel availability, electrolyte category, and working temperature [5]. Low-temperature fuel cells include DMFC, PEMFC, AFC, and PAFC. A comparison of fuel cell types for the concept selection process is shown in Table 1 [6–9]. Among them, the PEMFC technology has the potential to achieve higher efficiency than internal combustion engines at a lower operating temperature. Despite the fact that there are various types of fuel cells, this paper focuses on the performance of the proton exchange membrane (PEM) fuel cell type only. Accordingly, there are two types of PEMFC designs available in the market, and they are categorized based on their operations: low temperature operation is about 70–95°C and is known as PEMFCs (LT-PEMFCs), and high temperature PEMFCs operate around 120–250°C and are called HT-PEMFCs. Though LT-PEM fuel cells are in a transition between development and early commercialization because of their suitability for transport applications, this allows a healthy environment for researchers to solve important, fundamental problems. Hence, the focus of this paper is on the LT-PEM fuel cell only. Furthermore, for the Fuel cell electric vehicle (FCEV) there are many design influencing criteria as shown in Figure 2, however, fuel cell power is one of the significant parameter while configuring the vehicle performance parameters.

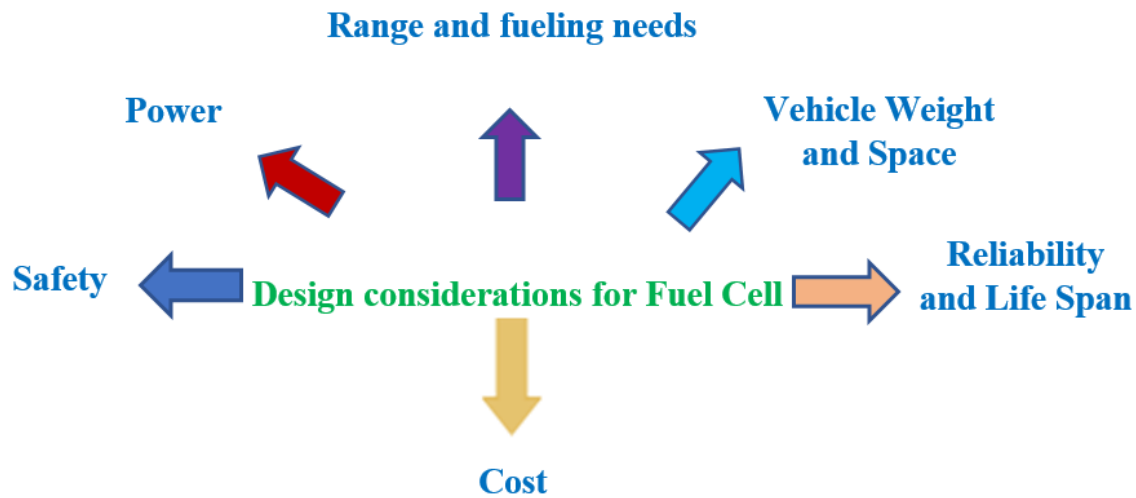


Figure 2. FCEV design influence criteria.

Accordingly, it will be difficult to run larger vehicles using power from the batteries alone. This is due to the need for more battery packs to meet the target vehicle mileage requirement as well as design challenges like packaging space constraints and weight. Hence, properly optimised fuel cell power is required based on fuel-cell electric vehicle tonnages. Though, for the large FCEV truck applications before developing the architecture, enormous FC powertrain testing is required on the one hand, and on the other hand, this will also involve cost and time [13]. Further, for this FCEV architecture, if smaller batteries are used, it will directly affect the range and power of the vehicle, and these are significant specifications for any commercial vehicle. As a result, several simulation studies are required to confirm the capabilities of the fuel cell, battery, and motor combined based on the vehicle's power requirements during gradient conditions and losses due to thermal, mechanical, and friction. It is also desirable to understand the FCEV boundary diagram while developing the FCEV architecture for simulation. Figure 3 shows a FCEV boundary diagram.

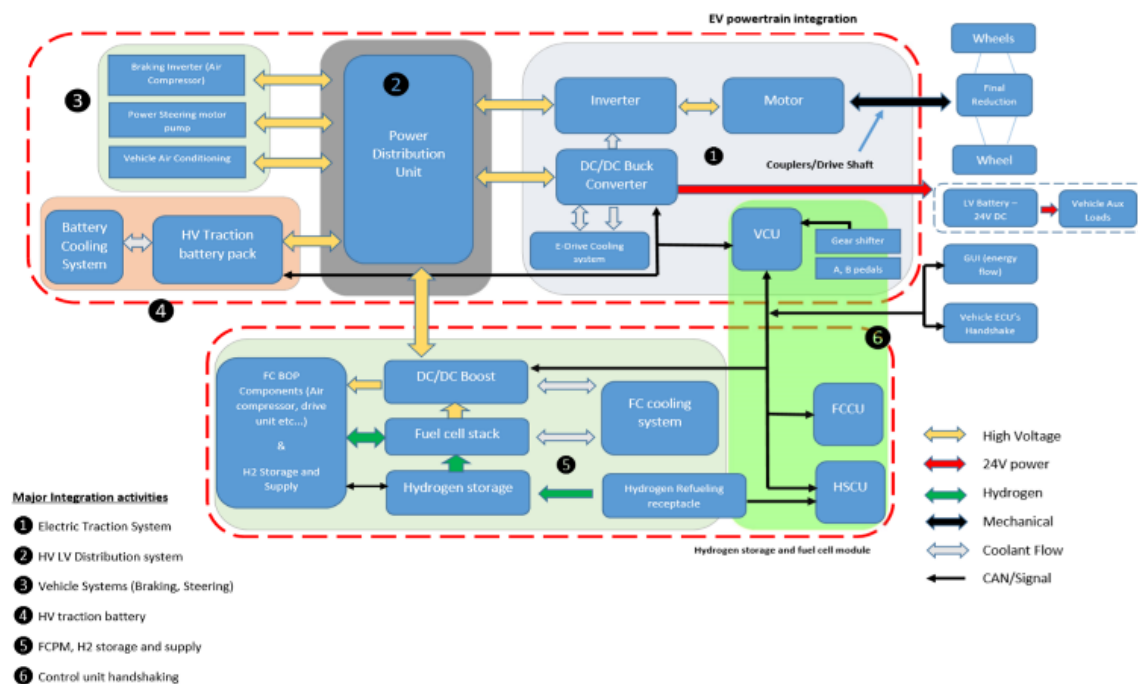


Figure 3. FCEV boundary diagram.

Moreover, for the fuel cell concept's formation, it is also critical to understand the PEM FC working mechanism as well as the gaseous transport of gases, protons, and electrons in a PEM fuel cell electrode. This PEMFC is typically composed of bipolar plates on both ends, a cathode gas diffusion layer, a membrane electrode assembly, and an anode diffusion layer. Figures 4a depict the basic schematic of LT-PEMFC. This type of polymer electrolyte membrane/proton exchange membrane (PEM) fuel cell is an electrochemical cell that combines hydrogen and oxygen to produce electricity, heat, and water. They are composed of a membrane electrode assembly (MEA) sandwiched between graphite anode and cathode flow field (FF) plates (Fig. 4a). A polymer membrane is sandwiched between anode and cathode electrodes in the MEA. Each electrode is composed of a catalyst layer (CL) composed of agglomerates of platinum particles, carbon grains, and ionomers, and a gas diffusion layer (GDL) composed of carbon paper.

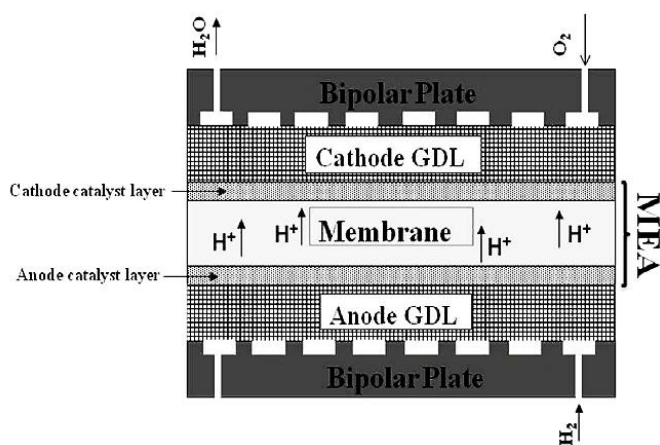


Figure 4a. Basic schematic of a LT-PEMFC.

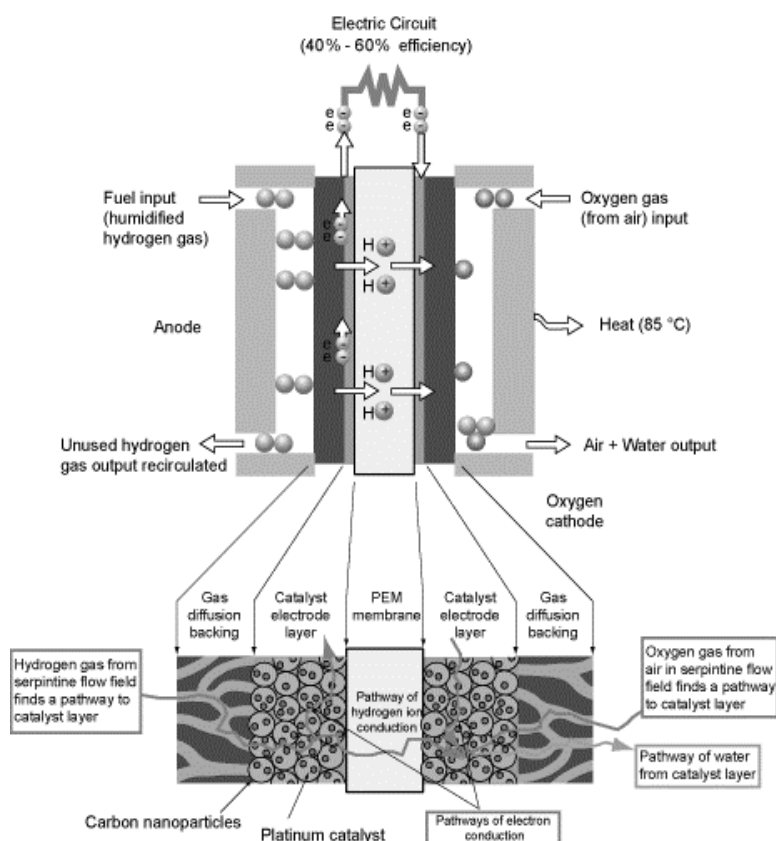


Figure 4b. Detailed layout of a LT-PEMFC.

In most cases, hydrogen gas is fed into the anode of a fuel cell and travels through the gas diffusion layer (GDL) to the anodic catalytic layer, where it is oxidised, resulting in proton transfer through the proton exchange membrane (PEM) and electron transfer through an external electrical circuit. Figure 4b shows the detailed layout of a LT-PEMFC. Concurrently, oxygen gas is introduced into the cathode, where it reacts with the protons and is reduced to water. Equations 1–2 [9] illustrate the anodic and cathodic reactions, along with the overall cell reaction.

Anode reaction:



Cathode reaction:



Furthermore, the transport of gases, charged species, and water can be better understood by closely inspecting the electrode structure [10]. Transport of gases, protons, and electrons in a LT-PEMFC is depicted in figure 5. An efficient PEM balances the transport processes needed for a fuel cell's function. The four required transportation processes are as follows:

1. The reactant and product gases are separated by the catalyst layer and the gas channels.
2. Electrons travel through the gas diffusion layer, which exists between the current collector and the catalyst layer.
3. Protons traverse the membrane and the catalyst layer.
4. Protons flow from anode to cathode across the membrane.

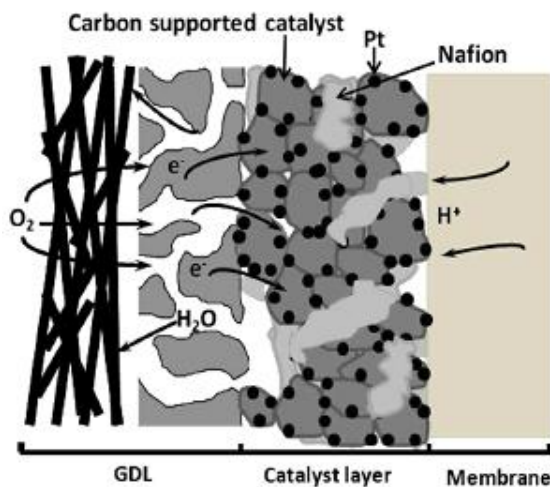


Figure 5. Transport of gases, protons, and electrons in a LT-PEMFC.

Typically, LT-PEMFCs are operated at temperatures below 100 °C due to the presence of both water vapour and liquid water, posing serious water management challenges. To avoid catalyst poisoning, LT-PEMFCs require highly pure fuel (hydrogen) with no or low impurities; the reformate gas must be treated using water gas shift and preferential oxidation processes to reduce CO content to below 10 ppm; and proper design to avoid restriction of oxygen mass transport at high current density will reduce large polarisation [11]. Further, this type of FC system has a short warm-up time for the smooth functioning of a fuel cell; however, consideration of several other factors such as ambient temperature, pressure, and humidity is also significant [12].

Overall, in this paper, a fuel cell electric vehicle architecture with >20 to 40 tonnes of tonnage using fuel cells, motors, and batteries is developed to simulate the fuel cell system's power performance for

meeting vehicle demand requirements. For this study, an FC electric vehicle model has been developed using GT-SUITE simulation software and is discussed below.

GT-SUITE SOFTWARE DESCRIPTION

Typically, for the design and simulation fuel cell electric vehicles, the primary objective is to have quick component selection and sizing based on the requirements. This software, with its productivity tools and multi-physical modeling capabilities, is observed to be suitable for optimizing, analyzing, and simulating fuel cells and their various subsystems. [14]. In addition, GT-SUITE is a dynamic simulation software with multi-function capabilities and pre-installed library templates for several automobile applications. This software is an effective tool to conceptualize and design systems and vehicle architectures to simulate conditions as close to the real world as possible. Furthermore, this software is also used to identify design flaws and determine the root cause of several problems. GT-SUITE is basically a multi-physics software to create models and systems based on the following libraries:

- Flow library (any fluid, gas, liquid, or mixture),
- Acoustics library (both non-linear and linear),
- Thermal library (all types of heat transfer),
- Mechanical library (kinematics, multi-body dynamics, frequency domain),
- The electric and electromagnetic libraries (circuits, electromechanical devices),
- chemistry (chemical kinetics) library
- signal processing control library
- It has built-in 3D CFD and 3D FE (thermal and structural).

Table 2. GT-SUITE simulation capability.

1	Fuel cell voltage power vs current density
2	Fuel Cell current density vs Time
3	Vehicle Speed vs Time
4	Vehicle displacement vs Time
5	Battery Voltage vs Time
6	SOC of battery vs Time
7	Battery C-rate vs Time
8	Battery power vs Time
9	Motor Torque vs Time
10	Motor efficiency vs Time
11	Motors losses vs Time
12	Motor power vs Time
13	Battery heat rejection rate vs Time
14	Motor speed vs Time
15	Fuel cell + Battery power vs Motor Power

Furthermore, this GT-SUITE is also capable of simulating the performance capabilities of the cooling system, the gas supply system to the cathode and anode, the humidification system, the hydrogen tank storage system, and the amount of H₂ fuel consumed by the fuel cell. The aforementioned system effectiveness can also be simulated across various steady-state and transient driving cycles [14]. This software is competent not only for designing the fuel cell system but also for integrating it with various other systems such as the heat management system, the DC/DC converter system, etc. In addition to the above, there are also verifications of various design parameters that can be simulated for fuel cell electric vehicles by using the GT-SUITE software, as shown in Table 2. Overall, this software provides the capability to design models ranging from 0D to 3D flawlessly for the users, and the fidelity of simulation can be adjusted within the model itself. This software can also be used to identify the thermal hotspots for a variety of systems and components using a 3D FE thermal discretization technique [14].

FUEL CELL ELECTRIC VEHICLE (20-40-TONNE) ARCHITECTURE

To understand the dynamics and performance of the real-world testing, this preliminary simulation study has been performed. For this study, a majority of the data for the fuel cell has been accumulated

based on a literature survey as well as vehicle specification data sheets. Though the data collected is as close as possible to real-world resources, this can be considered a valid assumption. In this paper, a 100 kW fuel cell is selected to simulate the fuel cell electric vehicle performance based on the vehicle power demand for a 20–40 tonne truck. The architecture of a fuel cell electric vehicle for this study is shown in Figure 6. This model has been developed using GT-SUITE software, and from the model, we can see that the fuel cell is connected to a DC-DC converter. A lithium-ion battery with a capacity of less than 55 kWhr is used to assist the fuel cell in delivering the power required by the motor during rapid acceleration and gradient conditions. Further, the fuel cell and the battery are connected to a motor (power > 200 kW), to meet the power demand requirements based on the selected vehicle tonnage.

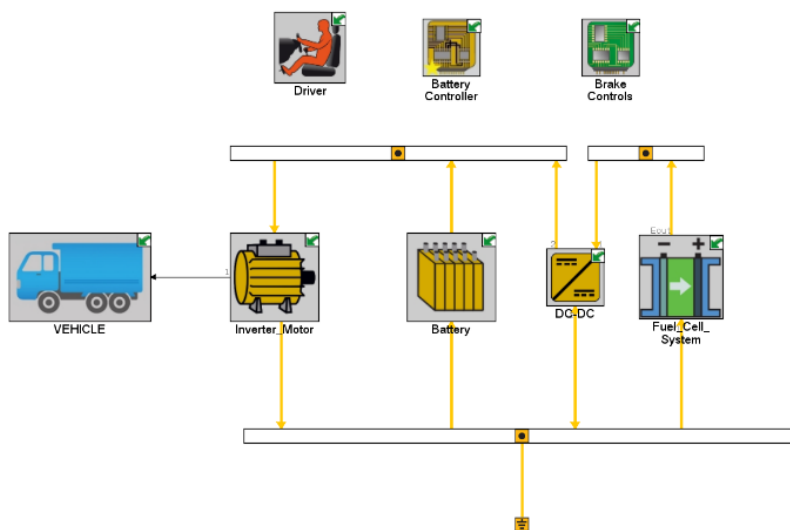


Figure 6. Fuel cell electric vehicle architecture.

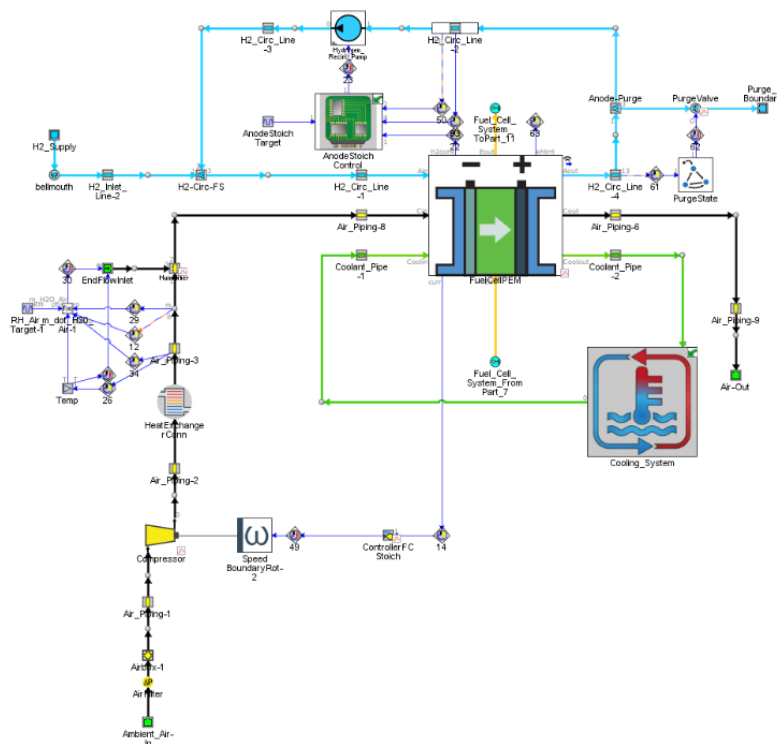


Figure 7. Fuel cell system simulation model.

Attribute	Unit	Object Value
Compressor Type		radial
External SAE File Name		ign...
Create Pre-Process Plots?		<input checked="" type="checkbox"/>
Pre-processing Message Level		simple
Reference Pressure	bar	1...
Reference Temperature	C	25...
Reference Gas Constant	J/kg-K	287...
Reference Ratio of Specific Heats		def (=1.4)...
Wheel Diameter	mm	34.7...

Figure 8. Compressor input data for simulation [15].

The fuel cell and its associated components model for GT-SUITE simulation is shown in Figure 7. For the FC stack cooling, a radiator system is connected separately, and for the DC-DC converter cooling, another radiator system is used. The hydrogen fuel delivery system is connected to the anode of the FC system, and the air inlet system with the compressor unit is connected to the cathode. The critical inputs for the compressor unit are given in Figure 8, while Figure 9 depicts the inputs for the heat exchanger unit and cooling system for the FC stack. Further, the motor input conditions are provided in Figure 10 for this simulation.

Attribute	Unit	Object Value
Diameter	mm	60...
Forward Discharge Coefficient		def...
Reverse Discharge Coefficient		def...
Imposed Fluid Temperature	C	70...
Heat Exchanger Outlet Temperature Ratio		ign...
Coolant Temperature	See Case...	[T_Coolant_init]...
Imposed Temperature Location		Downstream

Figure 9. Heat exchanger input data for simulation [15].

Attribute	Unit	Object Value
Efficiency / Power Loss		
<input checked="" type="radio"/> Electromechanical Conversion Efficiency		0.8766...
<input type="radio"/> Electromechanical Conversion Power Loss	kW	
<input type="checkbox"/> Include Inverter Losses		
Friction		
Friction Torque	N-m	ign...
Apply Friction during Zero Brake Request (No Electrical Draw)		<input type="checkbox"/>
Min / Max Torque Constraints		
<input checked="" type="radio"/> Define Min/Max Torque Curves		
Maximum Brake Torque		TractionMotorMaxTorque...
Minimum Brake Torque		TractionMotorMinTorque...
<input type="radio"/> Base Speed & Max Power		
Account for Torque Constraints During Direct Torque Control		<input checked="" type="checkbox"/>
Pre-Processed Plots		
Performance Maps		<input checked="" type="checkbox"/>

Figure 10. Motor input data for simulation.

RESULTS AND DISCUSSIONS

Steady State Simulation

To simulate the performance of a 20- to 40-tonne fuel cell electric truck under steady-state conditions, the GT-SUITE software is used. The steady state conditions are simulated for three vehicle speeds, such as 30, 50, and 70 kmph driving conditions. To stabilise all the parameters and ensure infallible results, each speed is simulated for 300 seconds. Based on the aforementioned scenario, simulated results will be discussed further.

The motor power demand for a fuel cell electric vehicle at a 30 kmph vehicle speed is shown in Figure 11. Based on this simulation study, motor power of >200 kW is required as per motor power demand. This could be accomplished from both power sources by producing about 72 kW of power from the fuel cell and >100 kW from the battery during the ramp-up speed conditions. Further, during the fully loaded conditions for the given 20-40-tonne vehicle, a ramp-up time of 12 seconds is achieved in simulation to reach the speed of 30 kmph. A peak is observed in the motor power; this could be due to the vehicle's demanded speed. Once the vehicle reaches the desired speed of 30 km/h, the motor power drops to a level suitable for cruising at the same speed.

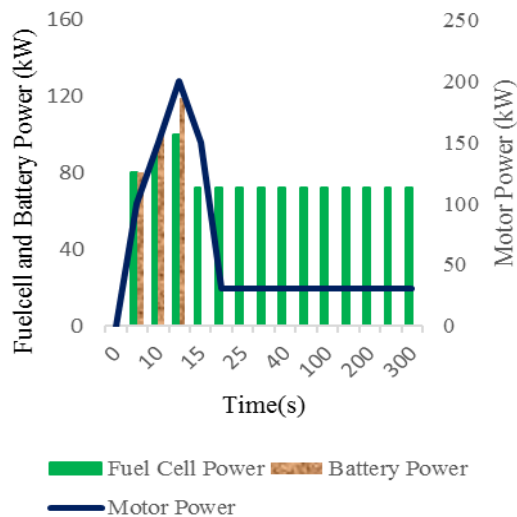


Figure 11. Motor power demand for a fuel cell electric vehicle travelling at 30 kmph speed.

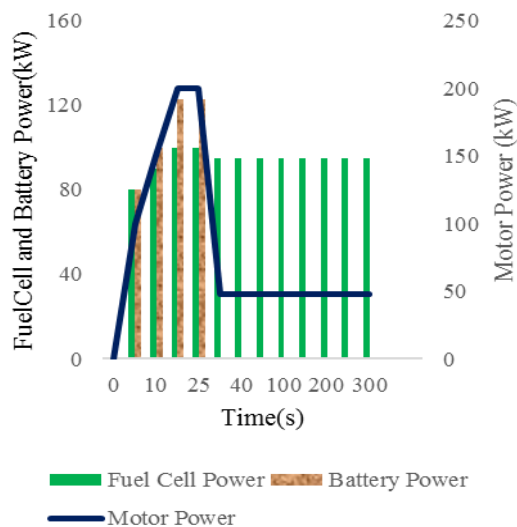


Figure 12. Motor power demand for a fuel cell electric vehicle travelling at 50 kmph speed.

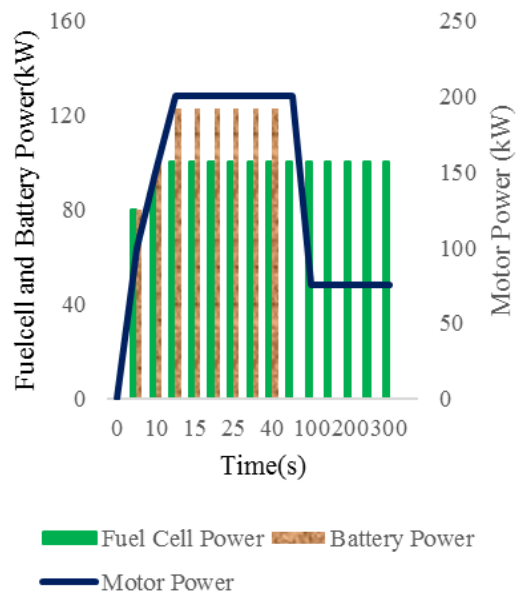


Figure 13. Motor power demand for a fuel cell electric vehicle travelling at 70 kmph speed.

The motor power demand for a fuel cell electric vehicle travelling at 50 kmph is given in Figure 12. Based on this simulation study, motor power of >200 kW is required to meet the motor demand. This could be accomplished by producing about 95 kW of power from the fuel cell and >100 kW from the battery during ramp-up speed conditions. Furthermore, under fully loaded conditions for the given 20-40-tonne vehicle, a ramp-up time of 25 seconds is required to reach the vehicle's speed of 50 kmph.

The motor power demand for a fuel cell electric vehicle at a 70 kmph vehicle speed condition is shown in Figure. 13. Based on this simulation study, motor power of >200 kW is required to meet the vehicle demand. This could be accomplished by producing 100 kW of power from the fuel cell and >100 kW from the battery during ramp-up speed conditions. Furthermore, under fully loaded conditions for the given 20–40-tonne vehicle, a ramp-up time of 50 seconds is required to reach the speed of 70 kmph. Overall, it can be seen that the motor power demand during acceleration is about 200 kW in all three vehicle speed conditions. However, after the vehicle reaches the desired speed range, it starts cruising consistently, and for this study, simulation is performed for 300 seconds at the given steady state condition. During the drop in motor power demand, excess power generated from the fuel cell is used for charging the battery.

The motor power comparison for different vehicle speed conditions is provided in Figure. 14. The time required to reach 30 kmph speed condition is less compared to 70 kmph. However, depending upon the vehicle acceleration conditions, the motor power selections must be optimised. For this 20-40-tonne vehicle application, this motor power selection is adequate to meet the required vehicle speed conditions.

The motor torque developed during the steady state condition is shown in Figure 15. The selected motor can provide more than 1000 Nm of torque during acceleration to meet 70 kmph vehicle speed conditions, and this torque is adequate for a 20- to 40-tonne vehicle's performance.

The motor speed developed during the steady state condition is shown in Figure 16. The selected motor is capable of providing a speed greater than 4000 rpm during acceleration for a 70 kmph vehicle at specified time conditions, and this speed is adequate for achieving the required vehicle performance for a 20–40-tonne vehicle.

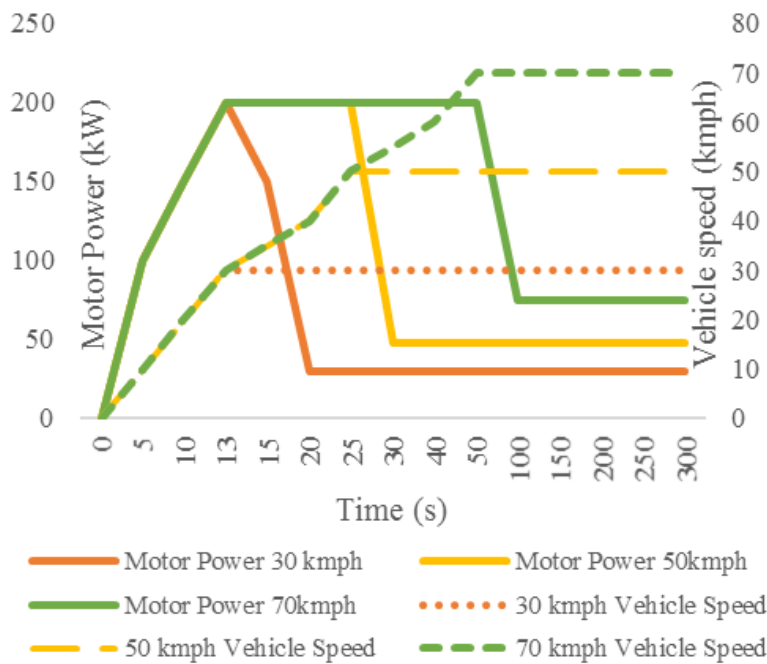


Figure 14. Motor power comparison for different vehicle speed conditions.

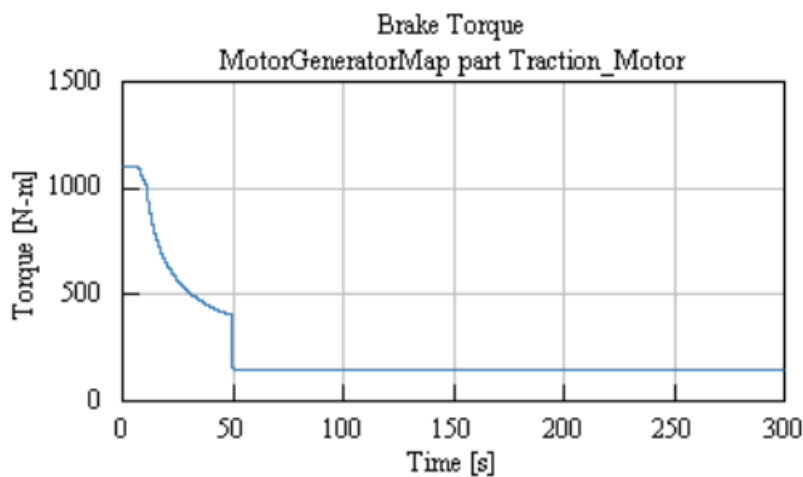


Figure 15. Motor torque during steady state cycle.

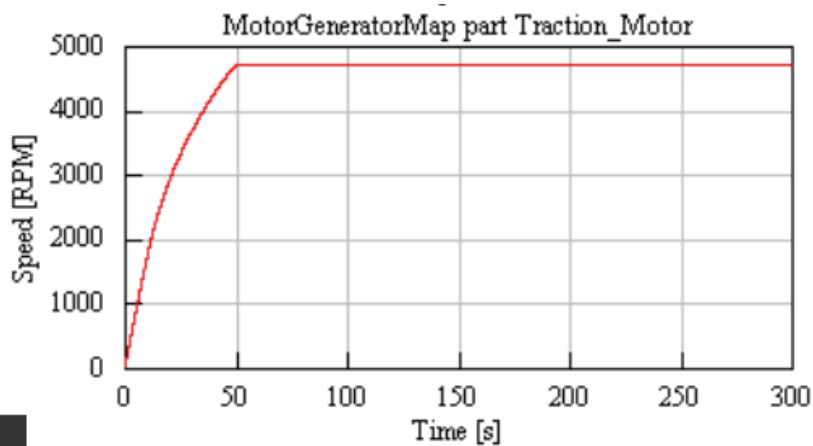


Figure 16. Motor speed during steady state cycle.

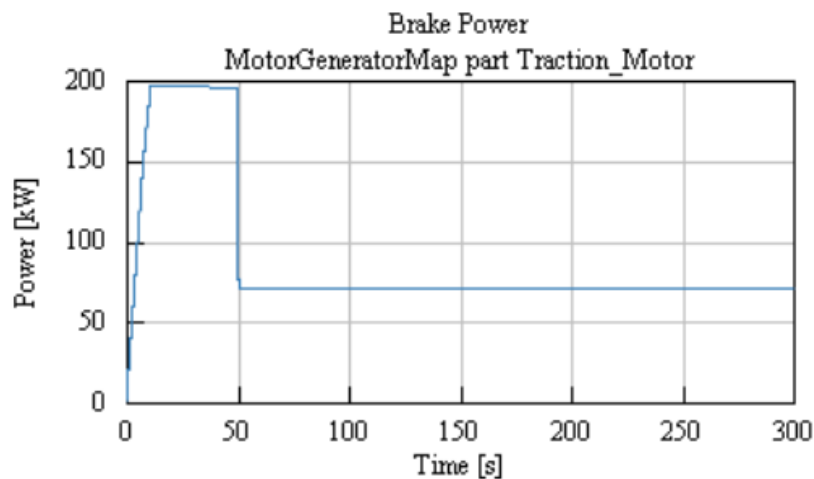


Figure 17. Motor power during steady state cycle.

The motor power developed during the steady state condition is shown in Figure 17. The selected motor is capable of providing power of around 200 kW during acceleration for a 70 kmph vehicle at the specified time conditions, and this power is adequate for a 20-40-tonne vehicle.

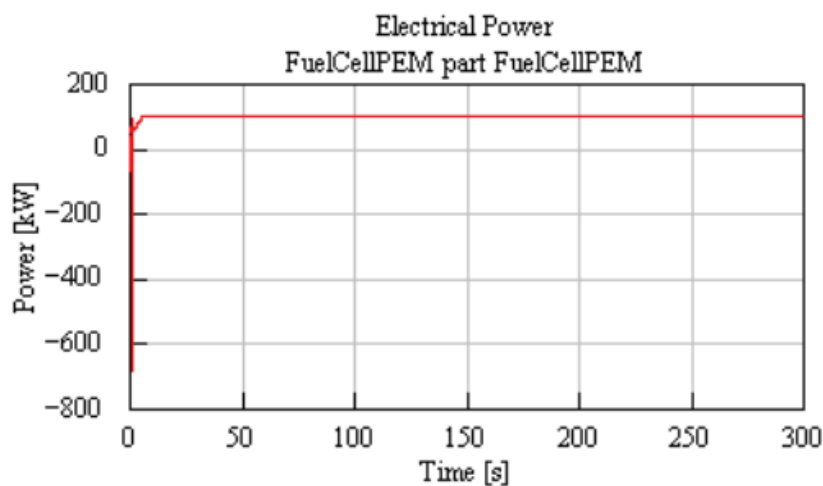


Figure 18. Fuel cell power during steady state cycle.

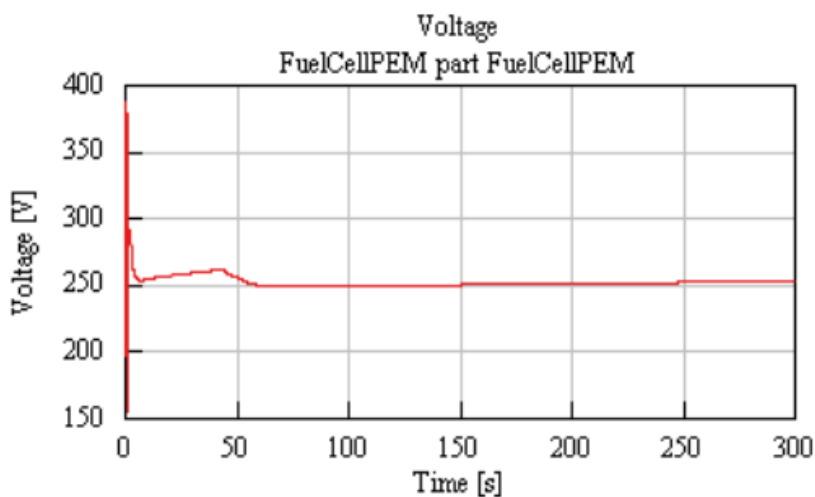


Figure 19. Fuel cell voltage during steady state cycle.

The fuel cell power developed during the steady state cycle is shown in figure 18. At 70 kmph, to meet the required motor power of 200 kW, the selected fuel cell system can provide around 100 kW of power. However, the excess power required for the motor will be provided by the battery. Overall, the selected proton exchange membrane technology and fuel cell associated operating parameters selection is adequate to meet the required fuel cell power according to the vehicle operating conditions.

The fuel cell power developed during the steady state cycle is shown in Figure 19. The selected fuel cell system provides around 250 volts; to increase this voltage, a DC-DC boost converter is used.

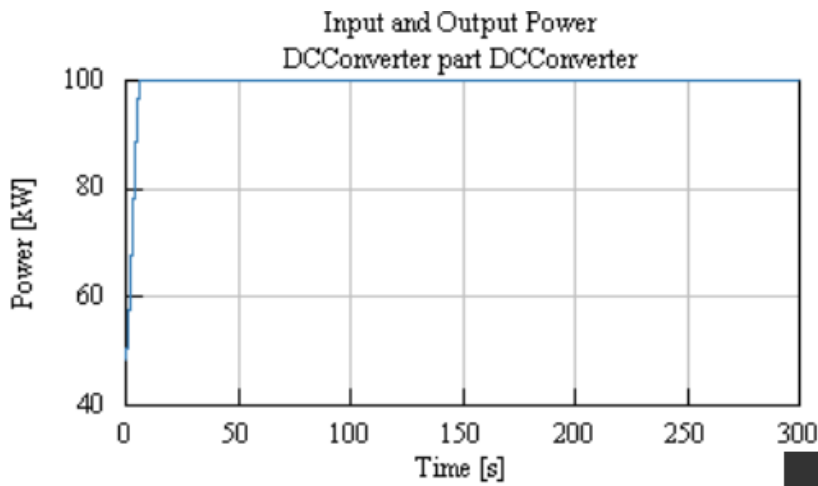


Figure 20. Fuel cell power after DC-DC out during steady state cycle.

The fuel cell power developed during the steady state cycle is shown in Figure 20. By increasing the aforementioned fuel cell voltage with DC-DC boost converter, the fuel cell power will be increased proportionally provided that the current should be kept constant. Overall 100 kW power from fuel cell system is achieved.

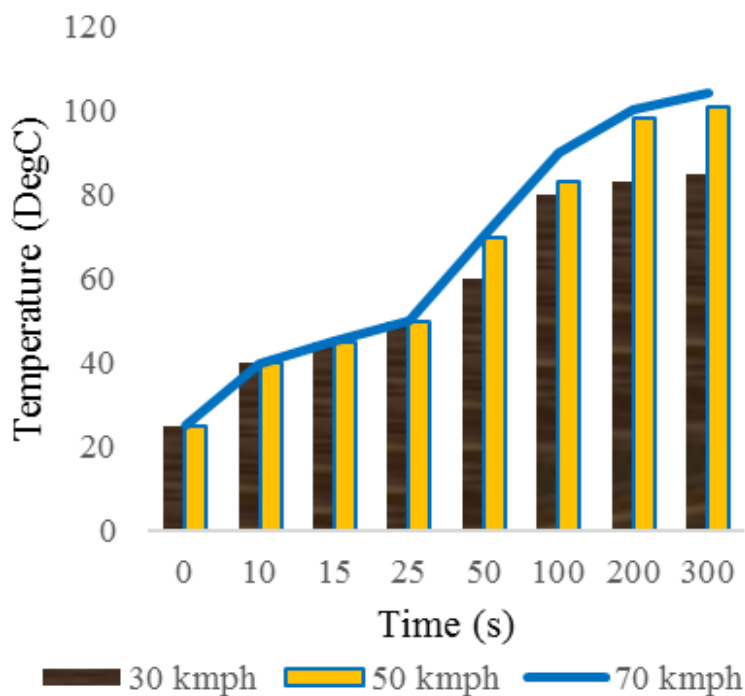


Figure 21. Fuel cell stack temperature comparison curve.

The fuel cell stack temperature comparison for three different vehicle speed conditions is shown in Figure 21. For the 30 kmph cruising speed, the fuel cell is continuously producing about 72 kW of power, and a stack out temperature of 85°C is observed in the simulation. Though the desired threshold temperature is 80°C for the fuel cell stack's enhanced operation, the observed temperature is marginally higher. Further, at 50 and 70 kmph cruising speeds, the fuel cell will continuously produce about 95 kW and 100 kW of power, respectively, and this will further increase the fuel stack out temperature. Due to the fuel cell stack's increased temperature, it is anticipated that the life of the fuel cell will drastically reduce, leading to concerns related to the membrane drying up and an efficiency drop. Hence, further modifications to the radiator system are required to enhance fuel cell performance. Overall, from the simulation, about 70 kW of continuous operating power is the optimum range for the selected fuel cell cooling system. However, to operate with the increased FC power range, modifications related to the cooling system are a must.

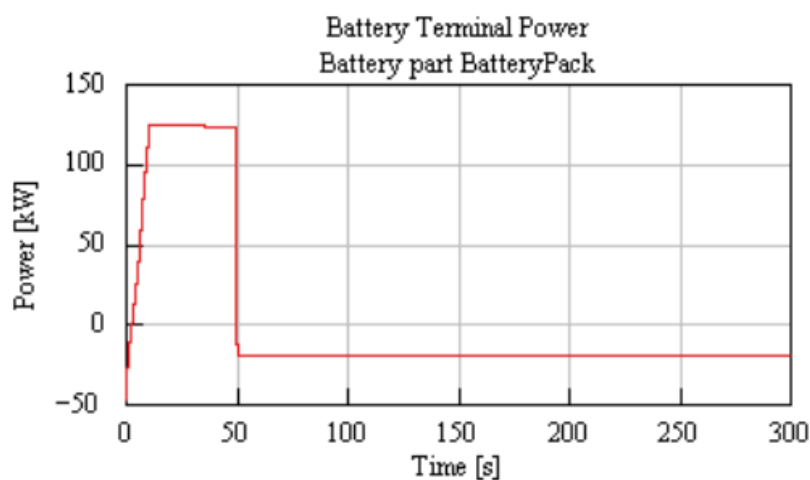


Figure 22. Battery power during steady state cycle.

Battery power during the steady state cycle is shown in Figure 22. The selected battery system is capable of providing additional power compared to fuel cell power to meet the overall motor power demand requirements. The selection of battery should also consider the thermal losses to meet vehicle requirements. Accordingly, the selected battery specification is adequate to meet the performance requirements of a 20–40-tonne vehicle.

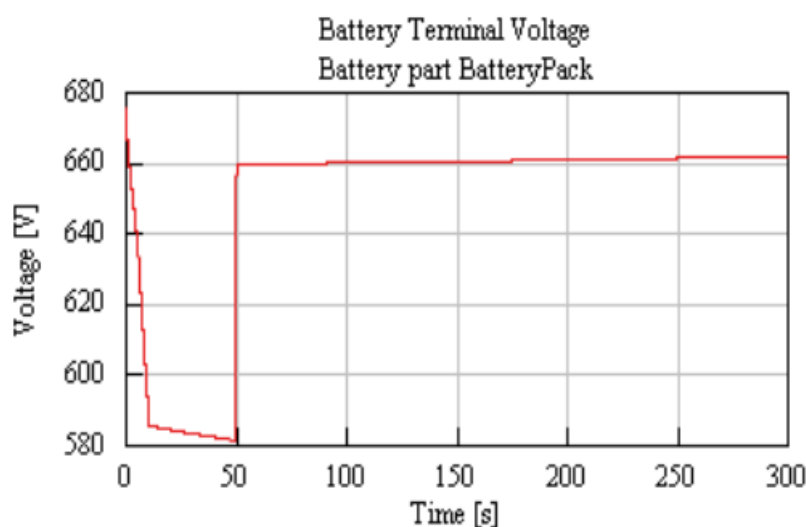


Figure 23. Battery voltage during steady state cycle.

The battery voltage during the steady state cycle is shown in Figure 23. The selected battery system can provide around 650 volts, and this voltage is used by the fuel cell system. Overall, this voltage is adequate to start the fuel cell system during key-on conditions.

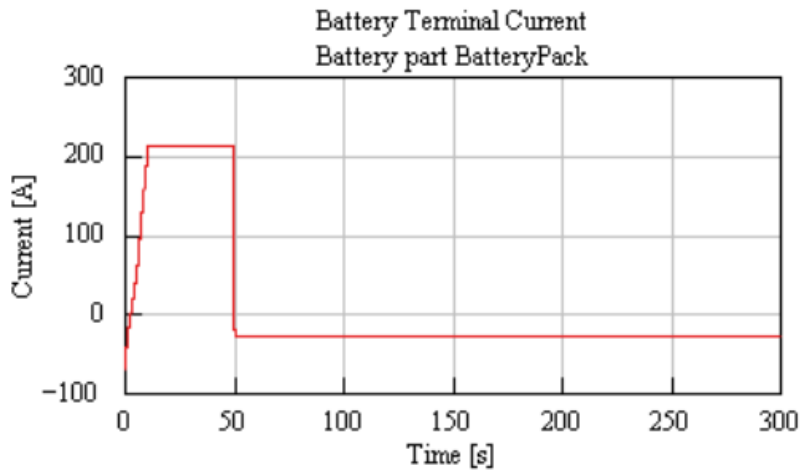


Figure 24. Battery current during steady state cycle.

The battery current during the steady state cycle is shown in Figure 24. The higher the current, the more work it can do at the same voltage. Therefore, the selected battery current specification is adequate to meet the performance requirements of a 20- to 40-tonne vehicle.

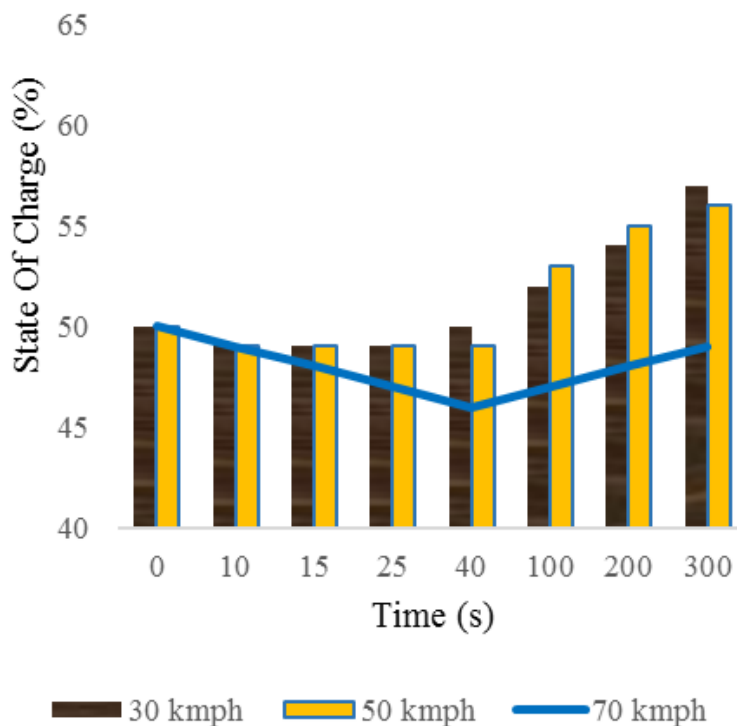


Figure 25. Battery state of charge comparison curve.

The battery state of charge comparison for three different vehicle speed conditions is shown in Figure. 25. In this simulation study, the battery SOC is assumed to be at 50 percent at the start of the simulation. During the sudden ramp-up to meet the motor demand of about 200 kW, the battery SOC can be seen dropping during initial acceleration in all three vehicle speed conditions. Until the vehicle reaches the

desired speed, the battery state of charge can be seen dropping marginally in all three vehicle speed conditions. During rapid acceleration, the battery state of charge (SOC%) drops and gradually begins to recharge during steady-state cruising. However, after reaching the desired vehicle speed, the battery gets recharged by the excess power from the fuel cell. Overall, the selected fuel cell and battery specifications for a 20–40-tonne vehicle are effective in meeting the vehicle power demand requirements. For 30 kmph and 50 kmph, there is no significant drop in SOC% observed. However, at 70 kmph, a marginal drop in SOC is observed.

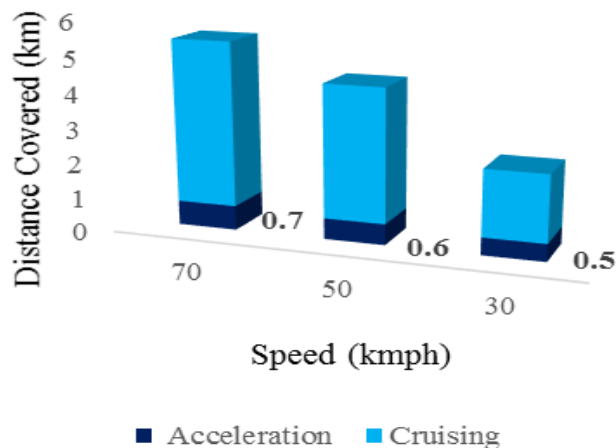


Figure 26. Vehicle travel distance comparison.

Vehicle travel distance comparison for three different vehicle speeds is shown in Figure 26. For the steady state simulation of 300 seconds at 30 kmph, this vehicle covers 0.5 km in 12.8 seconds. When compared with the 50 kmph steady state, the same vehicle covers 0.6 km in 25 seconds and 0.7 km in 50 seconds at 70 kmph. Though the distance travelled by a vehicle at constant speed is lower in the real world, it is still necessary to study the vehicle's behavior in a transient condition in order to verify the fuel cell performance based on the selected specifications.

Transient Simulation

Transient simulation is performed to understand the variations in power and temperature performance of the fuel cell and battery according to the transient motor demand conditions. This simulation study also provides a more realistic perspective on the performance of the 100 kW fuel cell under actual truck duty cycle conditions. The transient cycle chosen is a highway truck duty cycle, which is already available in the GT-SUITE software.

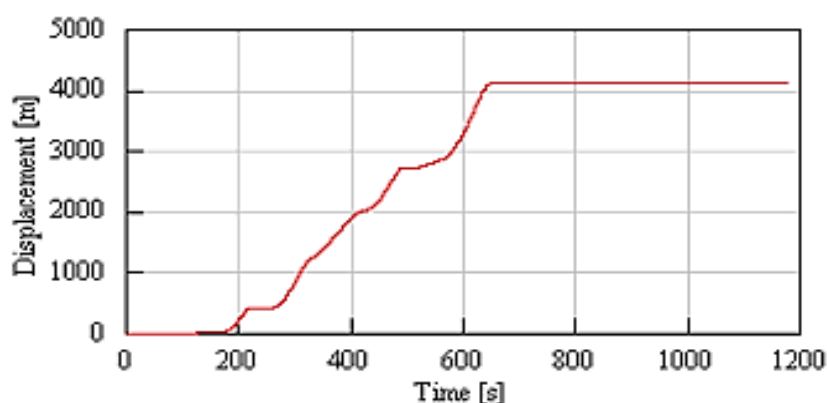


Figure 27. Vehicle displacement during transient cycle.

The vehicle displacement during the transient cycle is shown in figure 27. The overall cycle run time is 1200 seconds. The vehicle can be seen covering about 4.2 kilometers in 600 seconds. The selected highway truck duty cycle is capable of operating at about 70 kmph. Vehicle speed during transient cycle condition is shown in Figure 28. Based on the vehicle's operating duty cycle, the power demands for the, battery, and fuel cell are discussed below.

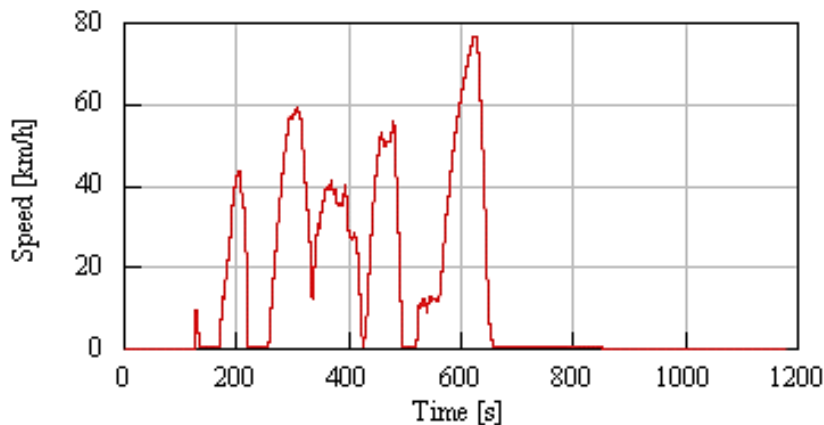


Figure 28. Vehicle speed during transient cycle.

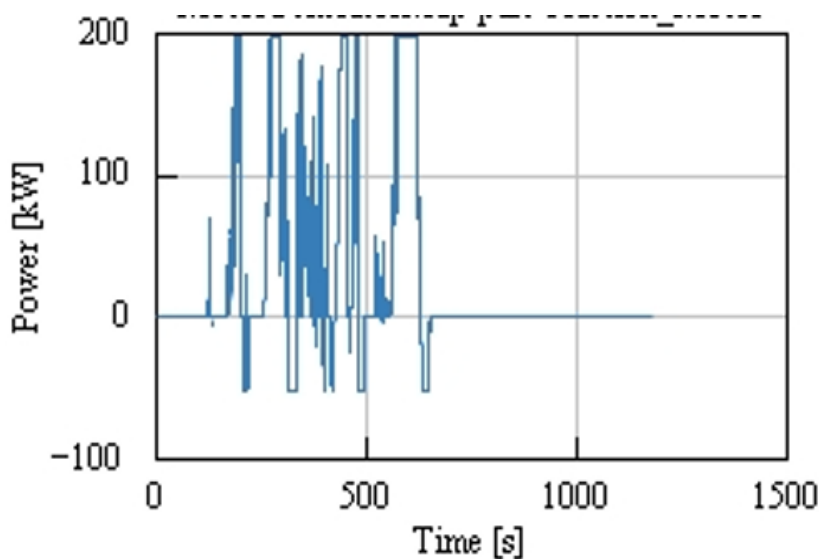


Figure 29. Motor power during transient cycle.

The power demanded by the motor during the transient highway cycle is shown in figure 29. The required power from the motor is about 200 kW for the maximum vehicle load of 20 to 40 tonnes while driving on the highway. Furthermore, there are also a few points where the motor power drops below 0 kW. This shows the area of regenerative braking where the regenerating motor power is supplied to the battery to raise its state of charge.

The battery power developed during the transient highway cycle is shown in figure 30. The selected battery system is adequate to provide more than 120 kW of power during truck duty cycle conditions to meet the required motor power demand of 200 kW.

The fuel cell power developed during the transient highway cycle is shown in figure. 31. The selected fuel cell system is adequate to provide 100 kW of power during duty cycle conditions to meet the required motor power demand of 200 kW.

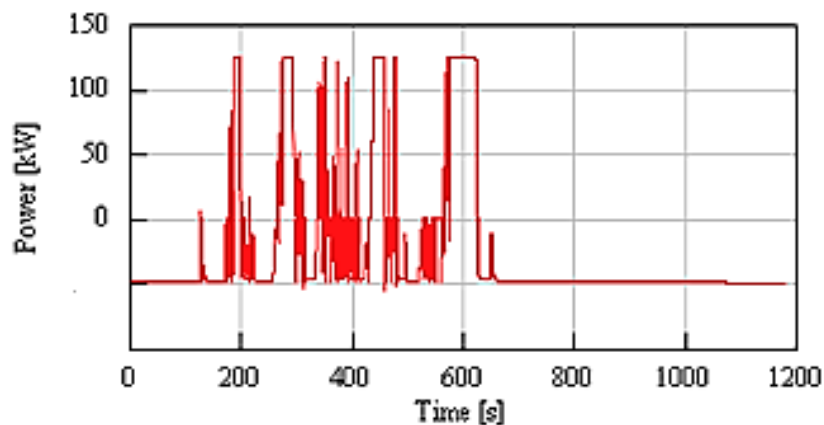


Figure 30. Battery power during transient cycle.

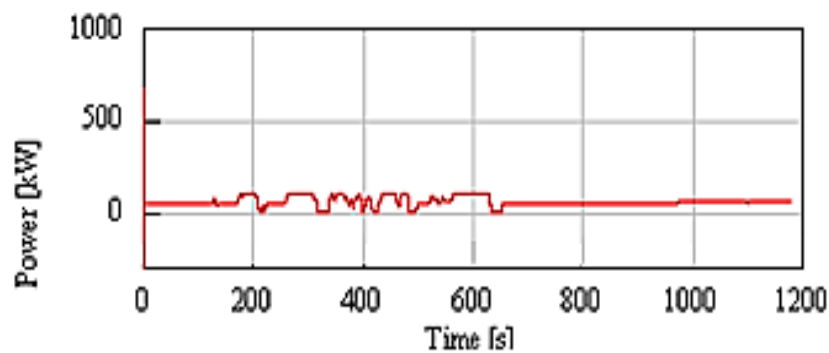


Figure 31. Fuel cell power during transient cycle.

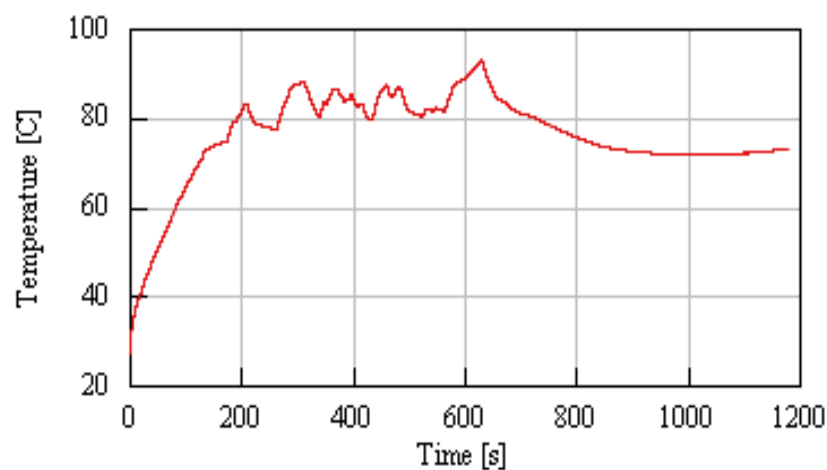


Figure 32. Fuel cell stack temperature during transient cycle.

The fuel cell stack out temperature during the transient cycle operating condition is shown in figure 32. During the start, the inlet coolant temperature is about 38 oC, and gradually, this temperature can be seen crossing the desired set boundary limit of 85 oC after 620 seconds at the coolant outlet. This could be due to heat exchange from the fuel cell stack based on prolonged maximum power production for the fuel cell. Overall, while pulling a 20- to 40-tonne vehicle during the transient cycle, it is anticipated that a 100 kW fuel cell has a high risk factor with the selected cooling system. As aforementioned, 70 kW of fuel cell power is the maximum and safest limit for continuous operation. Further, this power and temperature limitation can avoid membrane degradation due to overheating for the selected cooling system.

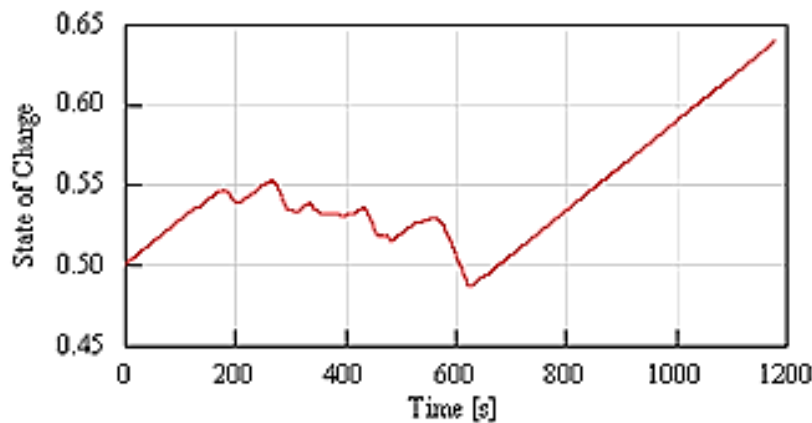


Figure 33. Battery SOC during transient cycle.

The battery SOC in a transient cycle is shown in figure. 33. During the highway duty cycle simulation, after 600 seconds, a rise in battery SOC is observed. When there is no power demand from the motor, the fuel cell can charge the battery until the SOC reaches 100%. However, the SOC can be seen increasing and decreasing throughout the cycle according to the motor power requirement during duty cycle operation.

CONCLUSIONS

Based on the GT-SUITE simulation technique, a fuel cell electric vehicle model has been developed using a 100 kW PEM fuel cell. Based on this simulation performance study with steady state as well as transient highway duty cycle scenarios, the capabilities of selected system specifications like power and cooling requirements for the fuel cell, motor, and battery are verified according to operating temperature and pressure considerations. This simulation study also reduced the number of preliminary tests required for finalising the fuel cell power specifications and limitations. It also provided an overview of the 100 kW fuel cell and its operating capabilities in 20- to 40-tonne truck vehicle applications with real-world scenarios in less time and at a lower cost.

REFERENCES

1. Mala, P.; Palanivel, M.; Priyan, S.; Anbazhagan, N. Acharya, S.; Joshi, G.P.; Ryoo, J. Sustainable Decision-Making Approach for Dual-Channel Manufacturing Systems under Space Constraints. *Sustainability* 2021, 13, 11456. <https://doi.org/10.3390/su132011456>.
2. Saikia, Kaustav & Kakati, Biraj & Boro, Bibha & Verma, Anil. (2018). Current Advances and Applications of Fuel Cell Technologies. 10.1007/978-981-13-1307-3_13.
3. Paul Breeze, Chapter 4 - The Proton Exchange Membrane Fuel Cell, Editor(s): Paul Breeze, Fuel Cells, Academic Press, 2017, Pages 33-43, ISBN 9780081010396, <https://doi.org/10.1016/B978-0-08-101039-6.00004-2>. (<https://www.sciencedirect.com/science/article/pii/B9780081010396000042>)
4. Cook B. Introduction to fuel cells and hydrogen technology. *Eng Sci Educ J* 2002; 11:205–16.
5. Kirubakaran A, Jain S, Nema RK. A review on fuel cell technologies and power electronic interface. *Renew Sustain Energy Rev* 2009; 13:2430–40.
6. Gregor H. Fuel cell technology handbook. New York: CRC Press; 2003.
7. Thounthong P, Davat B, Rael S, Sethakul P. Fuel cell high-power applications. *Industrial Electronics Magazine, IEEE* 2009;3:32–46.
8. Ellis MW, Von Spakovsky MR, Nelson DJ. Fuel cell systems: efficient, flexible energy conversion for the 21st century. *Proceedings of the IEEE*. 2001; 89:1808– 18.
9. Aquino, A.K., & Heng, J.O. (2017). Current and Temperature Distributions in a PEM Fuel Cell.
10. Feldhusen J., Schulz I., “Creating a holistic product development methodology by merging systems theory and dialectics”, TRIZ Future Conference 2007, www.sciencedirect.com, *Procedia Engineering* 9 (2011) 538–544.

11. S. Authayanun, M. Mamlouk, K. Scott and A. Arpornwichanop, *Appl. Energy*, 2013, 109, 192–201.
12. Jauregui-Becker J. M., Wits W. W., “An information model for product development: a case study at PHILIPS Shavers”, 2nd CIRP Global Web Conference, www.sciencedirect.com *Procedia CIRP* 9 (2013) 97 – 102.
13. Jiao J(R)., Chen C. H., “Customer requirement management in product development: A review of research issues”, *Concurrent Engineering: research and applications*, Vol. 14, No. 3, 2006
14. <https://www.mckinsey.com/industries/automotive-and-assembly/our-insights/how-hydrogen-combustion-engines-can-contribute-to-zero-missions>
15. Siddarth Srinivas, Evaluation of system simulation tools by modelling a 100 kW PEM fuel cell system, Chalmers University of Technology, Gothenburg, Sweden, Master’s Thesis, 2021.